This is a peer-reviewed, author's accepted manuscript of the following conference article:
Diaz-García, L., Reid, A., Jackson-Camargo, J., & Windmill, J. (2023). Directional passive acoustic structures inspired by the ear of Achroia grisella. Proceedings of Meetings on Acoustics, 50, [032001].
https://doi.org/10.1121/2.0001715

1. INTRODUCTION

There is currently a demand for microphones that are both small and directional. Their small size means they will be able to fit into portable applications like smartphones or hearing aids, providing ease of use and concealment to users; directionality implies that they are able not just to pick sound but also to favor sound coming from one direction and reject ambient noise coming from other directions. However, those two capacities are related through a trade-off. The way humans achieve directional hearing is by comparing the input received by each of our ears, different enough for our brain to perform the calculations and locate the source of the sound. If you reduce the space between the two ears, or microphones, too much, then sound will reach both at virtually the same time, with the difference not being enough to determine the origin of the stimulus. Classic microphone designs such as the condenser microphone are not suited for the task, which is why new, innovative models need to be considered.

Additive manufacturing, more commonly known as 3D-printing, has revolutionized engineering in the last few decades due to the ease and low cost of prototyping. With a Computer-Aided Design (CAD) software, one can quickly develop a personalized prototype with as much detail as one wishes. With materials, including the 3D-printer itself, being generally cheap, it is possible to produce an efficient prototype in any lab in a short time. With the current technology, it is possible to print thin membranes and diaphragms, which is a key component in microphone models.

A popular source of inspiration for such innovative microphones is the natural world, which received the name of bio-inspiration.[5,15,22,33] Insects are an example of living creature that face the very same challenge we described above. Directional hearing is desirable to find a potential mate or escape a predator, but insects' body size is usually small. The way insects overcome this challenge and achieve directional hearing is incredibly varied.[23] For example, *Ormia ochracea* is a parasitic fly with ultra-precise hearing known to have a complex inter-connected hearing system;[2,7,18] *Gryllus bimaculatus*, on the other hand, is a cricket with a tracheal system that connects to the outside of the body allowing sound to reach the inner side of their ears too.[17,24] These are just two examples, but different sorts of adaptations have been developed, and subsequently studied, to solve the issue of directional hearing at a small scale.

One such creature capable of directional hearing is the moth *Achroia grisella*.[3,10] *Achroia grisella* are also called lesser wax moth, and they are a small (average body size about 13 mm)[8] moth that parasites beehives. These moths belong to the *Arthropod* phylum, *Insecta* class, *Lepidoptera* order, and *Pyraloidea* superfamily. Like many nocturnal insects, the lesser wax moth is mainly preyed upon by bats, and are believed to have developed hearing in response to bat echolocation, to detect approaching bats and initiate evasive movements.[12,32] But for this end, *Achroia* does not need its hearing to be directional, it suffices to know that a bat is approaching and the moth will dive to the ground if flying or stop moving altogether if walking.

What is less common about *Achroia grisella* is that they further use their hearing for mating.[6,11] The male of the lesser wax moth emits a series of ultrasonic clicks with a structure at the base of their wings. The females are attracted by pheromones in the long distances, but in the close range, they listen for the song and zigzag until they reach it. Mechanisms like those of *Ormia* or *Gryllus* have been discarded in *Achroia grisella* through x-ray scans of their bodies.[19] Moreover, females with one ear pierced were still found able to track the artificial male calls,[27] which suggests that the moths' directional hearing is in fact monoaural and dependent exclusively on the morphology of the ear.

Achroia's hearing system consists of two ears that sit on the front of their abdomen next to each other. Each ear is comprised of an elliptical eardrum, with two sections of different thicknesses (the thicker one is called *conjuctivum* and the thinner one is called *tympanum proper* or tympanic membrane), and a *scolopidium*, a cluster of four auditory neurons that attach directly to the middle of the thin section.[13] When exposed to the mating call (main content of the signal approximately 100 kHz)[13,25,26], the eardrum moves in a complex, non-drum-like shape. There is a main amplitude peak close to, but not exactly on, the neuron attachment point. A ring of secondary peaks of lower amplitude surrounds the maximum. Lastly, there is a lower-amplitude, broader bump on the thicker section. All these sections move out of phase with each other, with the main peak almost in opposition to the other two regions.[19,21]

2. METHODS

The methodology followed combines different approaches and compares them between each other. Simultaneously, the model considered progressively increases its intricacy from a simplified version to a level of complexity closer to the real system. First, analytical equations were considered for the simpler cases that are not included in this paper; then, simulations were carried out with the Finite Element Modelling (FEM) software COMSOL Multiphysics; and lastly, samples were 3D-printed and measured in a 3D Laser Doppler Vibrometer. Good agreement was found between analytical results and simulation results for the simpler cases, thus validating the COMSOL model.

A. FINITE ELEMENT MODELLING

Finite Element Analysis was carried out in COMSOL Multiphysics®. A shell interface (Structural Mechanics module) is chosen to describe the system, accounting for a thin structure of significant bending stiffness. The physical characteristics of the system are parametrized to be easily changed to adapt the simulation to each considered case: values for the moth taken from the literature, measurements performed on 3D-printed samples, etc.

Two different kinds of study were performed: an eigenfrequency study and a general frequency study for directionality. The Eigenfrequency study is preset, and it is a straightforward way to obtain a number of natural resonances of a system.

For the directionality, a general frequency study is set, with an excitation stimulus consisting of a spherical wave of incident pressure field 1 Pa at one of the previously determined resonant frequencies. For producing polar plots, two angles were set, a polar angle and azimuthal angle. The azimuthal angle is the rise with respect of the ground and is set to 90 degrees to coincide with our setup (angle of the speaker surface with respect to the ground). The polar angle is swept over in intervals of 10 degrees, thus providing the points for the polar plot.

B. 3D-PRINTING

The 3D-printer used employs the Digital Light Projection (DLP) technique. DLP produces a 2D pixel array of each horizontal layer of the design, selectively exposing the photosensitive resin to UV light, which solidifies it. Each layer then attaches to the previous layers. If there is none, like in a suspended region or overhang, the exposure time will determine the thickness.[9] It is worth remarking that 3D-printing does present disadvantages, one of which is the difficulty of printing small samples due to residual stress gradients.[1,20,30,31] This can make it difficult to achieve repeatability and accuracy, which is why samples are measured individually to determine their size and thickness.

The material used is a custom mixed resin consisting of the base monomer, a photoinitiator, and a photo absorber. These are, in the same order, PEGDA (Polyethylene glycol diacrylate Mn 250), Phenylbis(2,4,6-trimethylbenzoyl)phosphine oxide at 0.5% weight percent, and Sudan I at 0.2% weight percent, purchased from Merck Life Sciences and used as bought. An ultrasonic bath (Decon FS250) was used to ensure even mixing of the three elements. From the literature, the Poisson's ratio and mass density of the resin are taken to be 0.32 and 1183 kg/m3 respectively.[28] The resin was calibrated in the following way: the UV light of the 3D-printer was shone directly onto the resin pool without a tray at different exposure times. The subsequent samples produced are stuck to the bottom of the resin pool, which are then carefully removed, washed in isopropyl alcohol, dried, and their thickness measured using a digital caliper. The relation of thicknesses and exposure times are adjusted using the model provided by Gong et al. [9]

C. X-RAY COMPUTER TOMOGRAPHY

To determine if the shape, size, and thickness of the 3D-printed samples is accurate, a Bruker Skyscan 1172 with SHT 11-megapixel camera and Mamamatsu 80 kV (100 mA) source is used. It generates images that are 1332 x 2000 px (resolution of 4.98 μm/px). Bruker's own CTvol software allows a volumetric reconstruction of the sample being scanned from the individual images.

Each image obtained is generated from the different attenuation across the sample. This is, likewise, dependent on the sample's absorption coefficient and thickness. The level of attenuation is significantly

less closer to an object's outer boundaries. The final measurement for the thickness will depend on this manual thresholding.

The sample for which results are presented was found to be 6.55 mm across the major axis, 4.95 mm along the minor axis, 102 μm of thickness in the thinner section and 259 μm of thickness in the thicker section. This agrees with the expected X-Y shrinkage and thicker curing of the Z layer thickness.

D. LASER DOPPLER VIBROMETRY

To measure the vibrations undergone by the structures printed, a 3D Laser Doppler Vibrometer (3D LDV) is employed. The machine is an MSA-1-3D scanning head (Polytec, Waldbrom, Germany), with sub-picometer amplitude resolution for in-plane and out-of-plane movements (provided by manufacturer). Measurements taken in the LDV are complex averaged five times.

For both frequency and directionality measurements, the plates are excited using a Labo LB-PS1401D speaker (frequency response of 80 Hz to 20 kHz, maximum output power of 60W, sensitivity of 88 dB, from manufacturer's specifications). The 3D LDV provides a visualizer software that shows out-of-plane vibrations over time, which are compared against theoretical resonances to identify them.

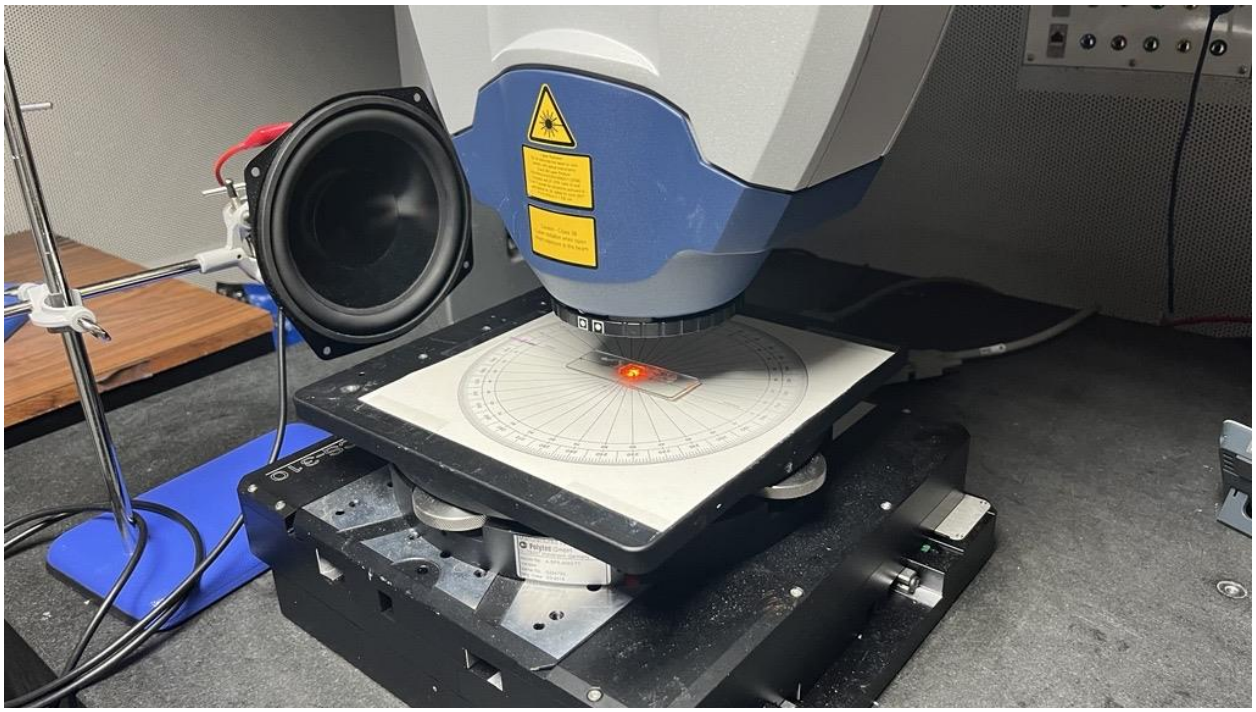

Fig 1. Experimental setup for the acquisition of the frequency and directivity responses. The sample is on a glass slide which can be rotated at measured intervals.

3. RESULTS

According to the analytical equations for a simple elliptical plate, resonant frequencies are proportional to Young's Modulus and thickness and inversely proportional to surface area. The resonant frequencies for a uniform elliptical plate are:

$$f_{m,n} = \frac{2 \cdot q_{m,n}}{\pi \cdot (a^2 - b^2)} \cdot \sqrt{\frac{D}{\rho \cdot h}}, m = 0,1,2 \dots, n = 1,2,3 \dots \quad (1)$$

Which depend on the eigenvalues ($q_{m,n}$), the major and minor semi-axes (a and b respectively), flexural rigidity (D), mass volume density (ρ), and thickness (h). The definition of D is the following:

$$D = \frac{E \cdot h^3}{12 \cdot (1 - \nu^2)} \quad (2)$$

Where the parameters not previously mentioned are as follows: Young's modulus (E), and Poisson's ratio (ν).[14] Although their exact values for *Achroia grisella* are not known with certainty, they are approximated as 1 GPa, 1180 kg/m^3 and 0.35 respectively. These values are obtained from literature values for insect cuticle.[29] Thickness is taken from literature or directly measured on the 3D-printed samples later on.[19] Even though the sample printed has two halves of different thicknesses, it is safe to assume we can expect a similar dependence with thickness and sizes of the axes.

Young's modulus was measured in two different ways for the custom material mix. The first one is through printing single layer cantilevers with our samples and examining their frequency response. The following equation from beam theory for a rectangular cantilever is used:

$$E = \frac{48 \cdot \pi^2 \cdot f_n^2 \cdot \rho \cdot L^4}{\lambda_n^4 \cdot h^2}, n = 1,2,3 \ldots \quad (3)$$

Where the parameters are mass volume density (ρ), the eigenfrequencies (f_n), the length of the beam (L), the eigenvalues (λ_n) and the thickness (h). [16] With all other values being known, Young's modulus is found to be 45.4 MPa. The second method used for measuring Young's modulus is compression testing, which provides the value of 53.0 MPa, obtained from the linear part of the stress-strain curves. Additionally, a value for the same custom resin's Young's modulus is also found in the literature as 52.9 MPa.[28] All values are found to be in reasonable agreement, and the value provided by the compression testing is chosen to be included in the COMSOL simulation.

A. FREQUENCY RESPONSE

The data obtained with the Laser Doppler Vibrometer for the sample mentioned in section 2.C was exported and plotted in MATLAB. The results can be seen in Figure 2. There is a large peak at approximately 1.7 kHz which is suspected to be a resonance of some element in the room; the reason for considering this point spurious is that this peak is present in all measurements of different setups and not just in this experiment. If the corresponding mode shape is observed, the whole structure can be seen vibrating up and down, as opposed to the actual relevant measurements where the edge remains clamped and only the central part of the membrane moves. Such is the case of the maxima at 9.506 kHz and at 11.788 kHz. The directivity response at these frequencies is evaluated in the next section.

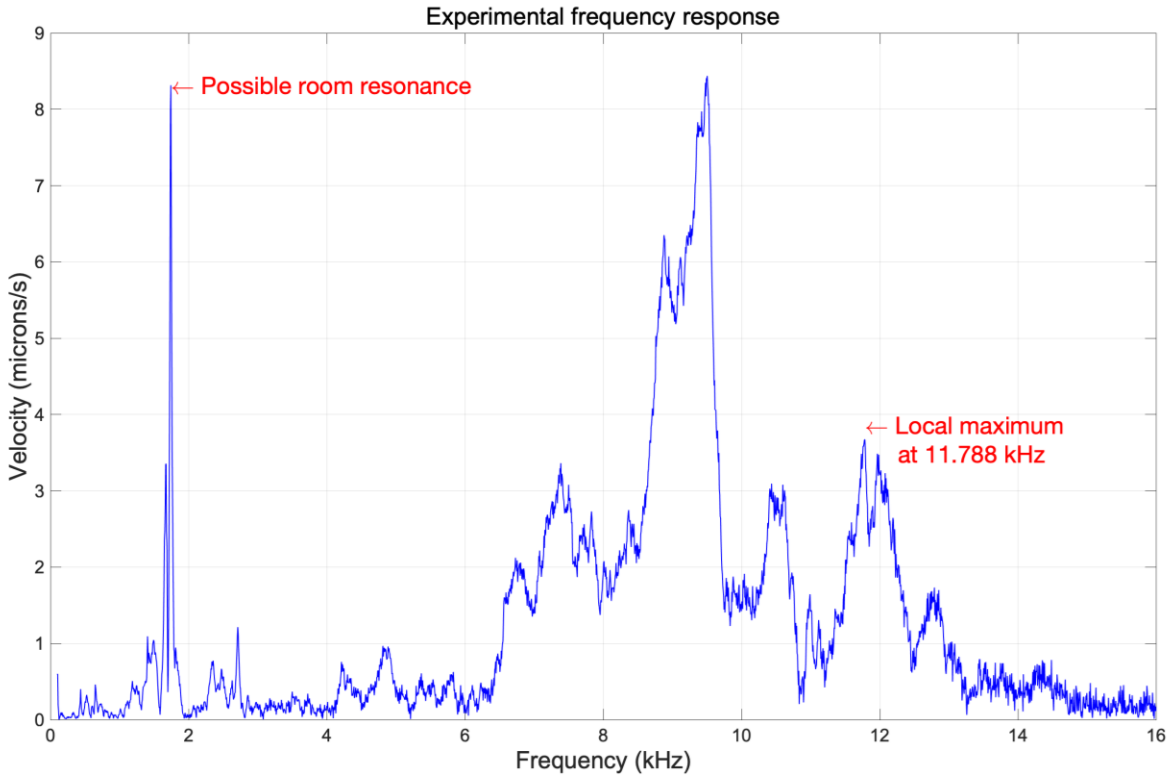

Fig 2. Frequency response obtained experimentally measuring at the approximate neuron attachment point. A broadband chirp produced by a speaker is used to excite the sample. The location of a spurious peak and the resonant frequency for which directivity will be evaluated are tagged in red.

B. DIRECTIVITY RESPONSE

The directivity responses for both 9.506 and 11.788 kHz are examined, and the one corresponding to 11.788 kHz is found to be a more recognizable shape to contrast against the simulation. Once a particular resonant frequency has been chosen from the frequency response, the COMSOL model is evaluated again with the parameters adjusted to fit the sample, in search of an eigenfrequency that is located close to the experimentally found resonant frequency. In this case, the eigenfrequency 10.026 kHz is found. The difference between resonant frequencies can be explained due to local irregularities in the 3D-printed sample, which are clearly seen under the microscope. An alternative manufacturing method might provide a more reliable result, but the cost and time of production would be higher. The simulated and experimentally obtained directivity patterns are then contrasted, a side-by-side comparison of the two can be seen in Figure 3. Both patterns present lobes pointing to what correspond to the sides of the moth (the setup is such that 0º is where the head of the moth is pointing to and 180º is the rear). The irregularities on the left side of the experimental pattern can be due to misalignment of the setup and/or human error in the measurements. Nonetheless, both patterns show directionality and are in good agreement with each other.

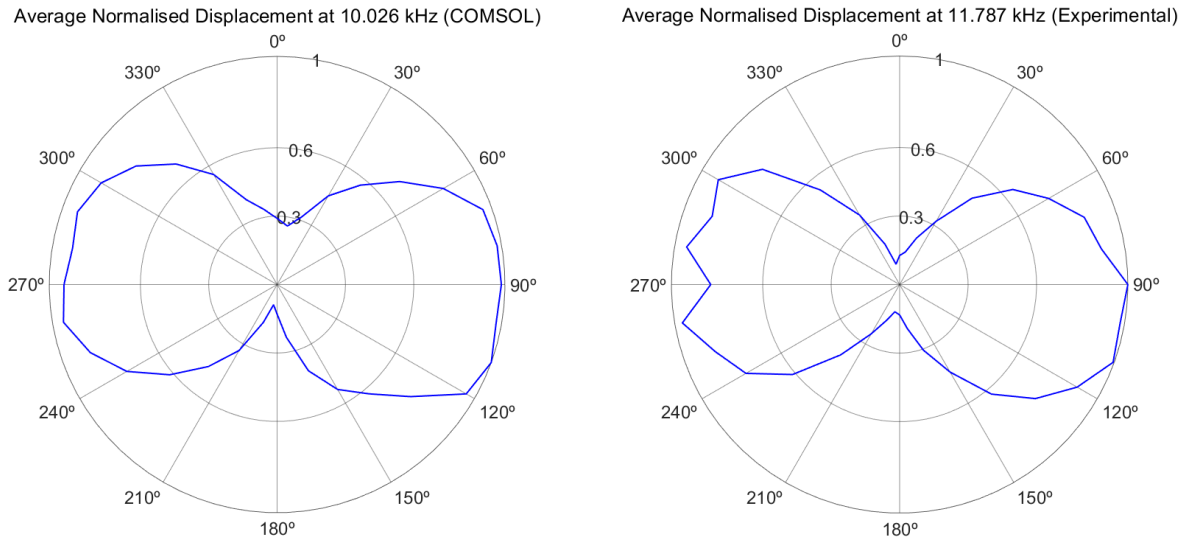

Fig 3. Directivity response obtained from COMSOL at 10.026 kHz (left) and experimentally at 11.788 kHz (right) for the sample described in section 2.C.

4. CONCLUSION

The 3D-printed sample shows clear passive acoustic directionality due to its asymmetrical morphology. It is seen that the experimentally measured directivity response agrees very well with what is expected from the simulations. Even though the pattern observed for the sample at this particular resonant frequency is not immediately advantageous for directional microphone manufacturing (a sideways bi-directional or figure-8 pattern), it is positive to see such good agreement and a modification of the setup could potentially be suitable for directional microphone applications. Previous studies of different patterns observed for lower resonant frequencies have been seen to possibly be helpful for the moth's directional hearing[4] and also show agreement with simulations.

Future work will look to produce the samples in piezoelectric materials to take the first step in the development of a novel bio-inspired transducer. Additionally, exploring different materials with other mechanical properties that bring down the resonant frequencies to the human audio range will also be investigated.

ACKNOWLEDGMENTS

The authors would like the acknowledge the help of Lisa Asciak in determining the Young's Modulus of the samples via compression testing.

REFERENCES

[1]P. S. Bychkov, V. M. Kozintsev, A. V. Manzhirov, and A. L. Popov, "Determination of Residual Stresses in Products in Additive Production by the Layer-by-Layer Photopolymerization Method," Mech. Solids **52**, 524–529 (2017). doi:10.3103/S0025654417050077

[2]W. H. Cade, M. Ciceran, and A. M. Murray, "Temporal patterns of parasitoid fly (Ormia ochracea) attraction to field cricket song (Gryllus integer)," , doi: 10.1139/z96-046. doi:10.1139/z96-046

[3]K. H. Dahm, D. Meyer, W. E. Finn, V. Reinhold, and H. Röller, "The olfactory and auditory mediated sex attraction in Achroia grisella (Fabr.)," Naturwissenschaften **58**, 265–266 (1971). doi:10.1007/BF00602990

[4]L. Díaz-García, A. Reid, J. Jackson-Camargo, and J. F. C. Windmill, "Towards a bio-inspired acoustic sensor: *Achroia grisella*'s ear," , doi: 10.1109/JSEN.2022.3197841. Presented at the IEEE Sensors Journal. doi:10.1109/JSEN.2022.3197841

[5]R. Domingo-Roca, B. Tiller, J. C. Jackson, and J. F. C. Windmill, "Bio-inspired 3D-printed piezoelectric device for acoustic frequency selection," Sens. Actuators Phys. **271**, 1–8 (2018).

[6]J. L. Eaton, *Lepidopteran anatomy*, (New York; Chichester; Brisbane, J. Wiley & Sons, 1988).
[7]R. S. Edgecomb, D. Robert, M. P. Read, and R. R. Hoy, "The tympanal hearing organ of a fly: phylogenetic analysis of its morphological origins," Cell Tissue Res. **282**, 251–268 (1995). doi:10.1007/BF00319116
[8]J. D. Ellis, J. R. Graham, and A. Mortensen, "Standard methods for wax moth research," J. Apic. Res. **52**, 1–17 (2013). doi:10.3896/IBRA.1.52.1.10
[9]H. Gong, M. Beauchamp, S. Perry, A. T. Woolley, and G. P. Nordin, "Optical approach to resin formulation for 3D printed microfluidics," RSC Adv. **5**, 106621–106632 (2015).
[10]M. Greenfield, and J. Coffelt, "Reproductive Behaviour of the Lesser Waxmoth, Achroia Grisella (Pyralidae: Galleriinae): Signalling, Pair Formation, Male Interactions, and Mate Guarding," Behaviour **84**, 287–314 (1983). doi:10.1163/156853983x00534
[11]M. D. Greenfield, "Acoustic Communication in the Nocturnal Lepidoptera," Animal Signals and Communication, in *Insect Hearing and Acoustic Communication*, edited by B. Hedwig (Berlin, Heidelberg, Springer, 2014) pp. 81–100.
[12]M. D. Greenfield, and M. Baker, "Bat Avoidance in Non-Aerial Insects: The Silence Response of Signaling Males in an Acoustic Moth," Ethology **109**, 427–442 (2003). doi:https://doi.org/10.1046/j.1439-0310.2003.00886.x
[13]L. Knopek, and C. Hintze-Podufal, "Uber den Bau der abdominalen Tympanalorgane der Kleinen Wachsmotte Achroia grisella (Fbr.)," Zool. Jahrbuecher Abt. Fuer Anat. Ontog. Tiere **1141**, 83–93 (1986).
[14]A. W. Leissa, *Vibration of Plates*, (Scientific and Technical Information Division, National Aeronautics and Space Administration, 1969).
[15]D. Mackie, J. Jackson, J. Brown, D. Uttamchandani, and J. Windmill, "Directional acoustic response of a silicon disc-based microelectromechanical systems structure," Micro Nano Lett. **9**, 276–279 (2014). doi:10.1049/mnl.2013.0677
[16]L. Meirovitch, *Analytical Methods in Vibrations*, (Macmillan, 1967).
[17]A. Michelsen, A. V. Popov, and B. Lewis, "Physics of directional hearing in the cricket Gryllus bimaculatus," J. Comp. Physiol. A **175**, 153–164 (1994). doi:10.1007/BF00215111
[18]R. N. Miles, D. Robert, and R. R. Hoy, "Mechanically coupled ears for directional hearing in the parasitoid fly Ormia ochracea," J. Acoust. Soc. Am. **98**, 3059 (1998). doi:10.1121/1.413830
[19]A. Reid, *Directional hearing at the micro-scale: bio-inspired sound localization*, (University of Strathclyde, 2017).
[20]A. Reid, J. C. Jackson, and J. F. C. Windmill, "Voxel based method for predictive modelling of solidification and stress in digital light processing based additive manufacture," Soft Matter **17**, 1881–1887 (2021). doi:10.1039/D0SM01968B
[21]A. Reid, T. Marin-Cudraz, J. F. Windmill, and M. D. Greenfield, "Evolution of directional hearing in moths via conversion of bat detection devices to asymmetric pressure gradient receivers," Proc. Natl. Acad. Sci. **113**, E7740–E7748 (2016).
[22]A. Reid, J. F. Windmill, and D. Uttamchandani, "Bio-inspired sound localization sensor with high directional sensitivity," Procedia Eng. **120**, 289–293 (2015).
[23]D. Robert, "Directional Hearing in Insects," Springer Handbook of Auditory Research, in *Sound Source Localization*, edited by A. N. Popper and R. R. Fay (New York, NY, Springer, 2005) pp. 6–35.
[24]J. Schul, M. Holderied, D. Von Helversen, and O. Von Helversen, "Directional hearing in grasshoppers: neurophysiological testing of a bioacoustic model," J. Exp. Biol. **202**, 121 (1999).
[25]H. G. Spangler, "Attraction of Female Lesser Wax Moths (Lepidoptera: Pyralidae) to Male-Produced and Artificial Sounds," J. Econ. Entomol. **77**, 346–349 (1984). doi:10.1093/jee/77.2.346
[26]H. G. Spangler, M. D. Greenfield, and A. Takessian, "Ultrasonic mate calling in the lesser wax moth," Physiol. Entomol. **9**, 87–95 (1984). doi:https://doi.org/10.1111/j.1365-3032.1984.tb00684.x
[27]H. G. Spangler, and C. L. Hippenmeyer, "Binaural phonotaxis in the lesser wax moth, Achroia grisella (F.) (Lepidoptera: Pyralidae)," J. Insect Behav. **1**, 117–122 (1988). doi:10.1007/BF01052508
[28]B. Tiller, A. Reid, B. Zhu, J. Guerreiro, R. Domingo-Roca, J. Curt Jackson, and J. F. C. Windmill, "Piezoelectric microphone via a digital light processing 3D printing process," Mater. Des. **165**, 107593 (2019). doi:10.1016/j.matdes.2019.107593
[29]J. F. V. Vincent, and U. G. K. Wegst, "Design and mechanical properties of insect cuticle," Arthropod Locomotion Systems: from Biological Materials and Systems to Robotics, Arthropod Struct. Dev. **33**, 187–199 (2004). doi:10.1016/j.asd.2004.05.006
[30]D. Wu, Z. Zhao, Q. Zhang, H. Jerry Qi, and D. Fang, "Mechanics of shape distortion of DLP 3D printed structures during UV post-curing," Soft Matter **15**, 6151–6159 (2019). doi:10.1039/C9SM00725C
[31]J. Wu, Z. Zhao, C. M. Hamel, X. Mu, X. Kuang, Z. Guo, and H. J. Qi, "Evolution of material properties during free radical photopolymerization," J. Mech. Phys. Solids **112**, 25–49 (2018). doi:10.1016/j.jmps.2017.11.018
[32]Y.-P. Zha, Q. Chen, and C. Lei, "Ultrasonic hearing in moths," Ann. Société Entomol. Fr. **45**, 145–156 (2009). doi:10.1080/00379271.2009.10697598
[33]Y. Zhang, R. Bauer, J. C. Jackson, W. M. Whitmer, J. F. Windmill, and D. Uttamchandani, "A low-frequency dual-band operational microphone mimicking the hearing property of Ormia ochracea," J. Microelectromechanical Syst. **27**, 667–676 (2018).